

Comparative study of models of Earth's magnetic field derived from Oersted, CHAMP and SAC-C Magnetic Satellite Data

Geeta Vichare and R.Rajaram

Indian Institute of Geomagnetism, Plot No-5, Sector-18, New Panvel. Navi Mumbai – 410 218
Email: geeta@iigs.iigm.res.in

ABSTRACT

The magnetic field near the earth contains contribution from three major sources, viz., main internal field that is due to electric currents in the outer core (97-99%), crustal field (1-2%), and external field (1-2%). The external field includes contribution due to ring currents, magnetotail, magnetopause currents and also subsurface currents induced by them. Over the past decade or so, there has been an attempt at "comprehensive modeling" that seamlessly integrates data collected over different epochs and different platforms to generate an integrated magnetic field model. It is found that the estimate of the contribution from ionospheric currents using satellite observations is sensitive to the Earth's magnetic field models, and hence it is essential to compare various magnetic field models. In the present work, we compare CHAOS model, the most recent long term model of Earth's magnetic field that uses Oersted, CHAMP and SAC-C satellite data with earlier epoch based models such as Oersted Initial Field Model, (OIFM) and CO2 models. CO2 model utilizes magnetic measurements from all three satellites as well as ground observatory data, whereas OIFM uses single satellite observations. While both CHAOS and CO2 models expand the static (core and crustal) field up to high order spherical harmonic ($n = 50$ and 49 respectively), OIFM has expansion only upto degree $n = 13$. The present study systematically separates and discusses the contribution from the various sources. The match between the internal field obtained from OIFM and CHAOS is found to be good in the longitudinal belt between 150°E and 250°E , indicating that in this longitude zone, the contribution due to the long wavelength crustal field is minimum. It is also observed that the difference between the internal field of OIFM and CHAOS is maximum along Indian and American sectors. Present work estimates the magnetic field variations due to the ring current, induced current, and magnetotail current, as well. It is found that the ring current contribution using OIFM is stronger compared to other two models. The external field due to ring current is discovered to be largest and that of due to the tail current is weakest. The effect of the tail current on the surface of the globe is found to be almost same everywhere, due to its far location. It is evident that in general, the ring current contributions are about five times stronger than that of due to the induced currents.

INTRODUCTION

The Earth is surrounded by an invisible force, which we call the magnetic field. The magnetic field originates deep within the Earth and extends many thousands of kilometers into space. The magnetic field near the earth contains contribution from three major sources: (i) Main internal field, (ii) Crustal field and (iii) External field

The maximum contribution to the geomagnetic field (97-99%) comes from the main internal field, which is due to electric currents flowing in the liquid outer core. It is believed to be caused by the

convection of molten iron, within the outer liquid core, along with a Coriolis effect caused by the overall planetary rotation that tends to organize currents in rolls aligned along the north-south polar axis. When conducting fluid flows across an existing magnetic field, electric currents are induced, which in turn creates another magnetic field. When this magnetic field reinforces the original magnetic field, a dynamo is created which sustains itself.

Second major source of earth's magnetic field is due to the presence of magnetized rocks in the crust and upper mantle, which produces "Crustal field" and its contribution is only $\sim 1-2\%$ of the total

geomagnetic field. Thus, the Earth's magnetic field, which originates inside the earth, is a superposition of the field generated by the geodynamo in the liquid outer core (main internal field) and the crustal field.

Third source is external field that includes contribution due to currents flowing in the ionosphere, magnetotail, and magnetopause. Charged particles trapped by the geomagnetic field in the magnetosphere, drift around the Earth at a distance of 3–8 R_E creating a westward electric ring current whose field opposes the main geomagnetic field (Daglis & Kozyra 2002). The strength of this field is of the order of tens of nT during quiet times and several hundred nT during magnetic storms. The symmetric part of this composite disturbance field is tracked by the Dst (disturbance storm-time) index (Sugiura 1964), derived from the measurements of four low latitude observatories. Ring currents flowing around the earth and their induced counter parts in the subsurface constitute major part of the external field. Currents flowing in the lower ionosphere, magnetopause, and magnetotail also produce magnetic field on the surface of the earth.

Beside these, there is Oceanic magnetic field also, generated due to ocean circulation, which is the most faintest.

It should also be noted that the main internal field is near dipolar and change is only 1% per year, while the external field varies on time scales of seconds to days, primarily due to the solar interactions.

The Earth's magnetic field models are obtained from the ground as well as satellite magnetic field measurements, normally for the period of five years. Satellite data has advantage over ground measurements in terms of its global coverage and hence the geomagnetic models based on satellite data are assumed to be more realistic. Measurements of on-board magnetic field have been started several decades ago. Twenty years after the Magsat mission, the Oersted satellite was launched on February 23, 1999 in a near polar orbit. Immediately after this, CHAMP satellite was launched in July 2000; and then SAC-C was put into orbit in 2001. All three missions carry essentially the same instrumentation and provide magnetic field observations from space with unprecedented accuracy. Oersted and CHAMP are still in orbit and providing magnetic field measurements, while scalar magnetometer of SAC-C was active until 2004. Thus, all these three satellites were in the orbit almost during the same period.

The orbital altitude of Oersted and SAC-C is ~ 700 km, and that of CHAMP satellite is ~ 450 km.

Due to the somewhat different altitudes and drift rates through the local time, these different spacecrafts sense the various internal and external field contributions differently.

Availability of huge amount of satellite data has lead to "Comprehensive Modeling", which focuses on the contribution from different sources that give rise to exclusive Crustal field model, Lithospheric field model (Maus et al., 2006, 2007), Oceanic magnetic field model (Maus & Kuvshinov 2004) etc. It also seamlessly integrates data collected over different epochs and different platforms to generate an integrated magnetic field model. As a result of this, several models of geomagnetic field have been proposed.

It is found that the estimate of the contribution due to the ionospheric currents (e.g. equatorial electrojet, Sq- solar quiet time currents) using satellite observations is sensitive to the Earth's magnetic field models (Jadhav, Raja Ram & Raja Ram 2002; McCreddie & Iymori 2006). Often, researchers working on the satellite data-based study of the ionospheric current systems face a dilemma in choosing among several models of the geomagnetic field. And hence it is very important to compare the magnetic field values obtained from various Earth's magnetic field models. In the present paper, we attempt to compare three widely-used, satellite-based geomagnetic field models.

GEOMAGNETIC FIELD MODELS:

Earth's main magnetic field can be described using Gauss coefficients derived from a spherical harmonic analysis (Chapman and Bartel, 1940). For the comparison, we use three geomagnetic field models with different features, which are briefly discussed in the following subsections.

Oersted Initial Field Model, (OIFM):

This is one of the very early satellite based geomagnetic field models derived from scalar magnetic field data obtained by Oersted satellite collected during the period between December 1999 and January 2000. A very convenient way of representing geomagnetic fields is to expand the scalar magnetic potential into spherical harmonic functions. Such a model can then be evaluated at any desired location to provide the magnetic field vector. The magnetic field vector $B = -\tilde{N}V$ is derived from a scalar potential V , which is expanded in spherical harmonics:

$$\begin{aligned}
 V = a \left\{ \sum_{n=1}^{13} \sum_{m=0}^n (g_n^m \cos m\phi + h_n^m \sin m\phi) \left(\frac{a}{r}\right)^{n+1} P_n^m(\cos\theta) \right. \\
 + \sum_{n=1}^2 \sum_{m=0}^n (q_n^m \cos m\phi + s_n^m \sin m\phi) \left(\frac{r}{a}\right)^n P_n^m(\cos\theta) \\
 \left. + Dst \cdot \left[\left(\frac{r}{a}\right) + Q_1 \left(\frac{a}{r}\right)^2 \right] \cdot \right. \\
 \left. [\tilde{q}_1^0 P_1^0(\cos\theta) + (\tilde{q}_1^1 \cos\phi + \tilde{s}_1^1 \sin\phi) P_1^1(\cos\theta)] \right\}. \quad \dots (1)
 \end{aligned}$$

Where, $a = 6371.2$ km is the mean radius of the Earth, (r, θ, ϕ) are geocentric coordinates with θ and ϕ as geographic colatitude and longitude respectively, $P_n^m(\cos\theta)$ are the associated Schmidt-normalized Legendre functions and (g_n^m, h_n^m) and (q_n^m, s_n^m) are the Gauss coefficients describing internal and external source fields, respectively. The coefficients $\tilde{q}_1^0, \tilde{q}_1^1$ and \tilde{s}_1^1 account for the Dst- dependent part of the external dipole. Thus, in equation (1) first term gives internal magnetic field, second term gives external field, and third term represents the Dst-dependent part of the external field. The internally induced counterpart of the external dipole is represented by the factor $Q_1 = 0.27$, a value found from Magsat data by Langel & Estes (1985). The physical description of this coefficient is given as follows:

The time varying magnetospheric fields induce electric currents in the Earth, which in turn give rise to a secondary internal field whose strength is roughly one third of the external field. Hence, the disturbance field observed at the Earth's surface is the sum of the external source field and its induced counterpart. If the Earth were an ideal conductor then the two fields would be exactly in phase because currents would be induced in such a way as to prevent any external field from entering into the conductor.

Note that the OIFM model includes internal main field coefficients to the order 13, secular changes to the order 8, an external field to degree 2, and Dst-dependent internal and external field correction up to degree 1 (Olsen et al., 2000).

CO2 Model:

CO2 model, which is a initial official CHAMP Main Magnetic Field Model (Holme et al., 2003) utilizes magnetic field measurements of all three satellites, viz., Oersted, CHAMP and SAC-C, as well as ground observatory data. This is again epoch-based model, employs data collected during the period between July 2000 and December 2001.

The magnetic potential is given by

$$\begin{aligned}
 V = a \sum_{n,m} (g_n^m \cos m\phi + h_n^m \sin m\phi) \left(\frac{a}{r}\right)^{n+1} P_n^m(\cos\theta) \\
 + a \sum_{n,m} (q_n^m \cos mT_d + s_n^m \sin mT_d) \left(\frac{r}{a}\right)^n P_n^m(\cos\theta_d) \\
 + a Dst(t) \cdot \left[\left(\frac{r}{a}\right) + Q_1 \left(\frac{a}{r}\right)^2 \right] \cdot [\tilde{q}_1^0 P_1^0(\cos\theta_d) + (\tilde{q}_1^1 \cos T_d + \tilde{s}_1^1 \sin T_d) P_1^1(\cos\theta_d)] \\
 \dots \dots K \quad (2)
 \end{aligned}$$

Here θ and ϕ are geographic colatitude and longitude respectively used for the internal field expansion, while θ_d and T_d are dipole colatitude and dipole local time (MLT) respectively, which are used for the external field calculations. The MLT is equivalent to the longitude in the solar magnetic coordinate system. The Q_1 factor representing the induced magnetic field is 0.28.

CO2 model includes internal field coefficients up to order 49 and linear secular variation of degree 13. The external field correction is made up to order 2.

CHAOS model:

This is the most recent long-term model of Earth's magnetic field that uses Oersted, CHAMP and SAC-C data (Olsen et al., 2006). CHAOS employs static field coefficients up to order 50 and linear secular variation of degree 18. This model also considers the effects of the magnetospheric ring current and induced currents, but in addition to these, it evaluates the effects of the magnetotail currents too.

In earlier two sub sections, we have expressed the magnetic scalar potential as a sum of the internal and external parts ($V = V^{int} + V^{ext}$). It should be kept in the mind that the mathematical expression for the internal part is same in all models, only the expansion coefficients and the maximum degree of spherical harmonic expansion is different. Therefore for CHAOS model, we do not write the internal field part, and show only the external potential, V^{ext} in equation (3), which describes large-scale magnetospheric sources.

$$\begin{aligned}
 V^{ext} = a \sum_{n=1}^2 \sum_{m=0}^n (q_n^m \cos mT_d + s_n^m \sin mT_d) P_n^m(\cos\theta_d) \left(\frac{r}{a}\right)^n \\
 + a \sum_{m=0}^1 (\tilde{q}_1^m \cos mT_d + \tilde{s}_1^m \sin mT_d) \left(Est(t) \left(\frac{r}{a}\right) + Ist(t) \left(\frac{a}{r}\right)^2 \right) P_1^m(\cos\theta_d) \\
 + a \sum_{n=1}^2 q_n^{0GSM} R_n^0(r, \theta, \phi) \quad \dots \dots K \quad (3)
 \end{aligned}$$

Here, θ_d and T_d are dipole colatitude and dipole local time, respectively (which are identical to colatitude and longitude in the solar magnetic coordinates system). Therefore the first two lines represent an expansion in the solar magnetic (SM) coordinate system and describe mainly contributions from the near magnetosphere, i.e. the ring current. The disturbance magnetic field, Dst, is decomposed into external and induced contributions provides the Est index for the external source field and the Ist index for the internal induced field ($D_{st}(t) = E_{st}(t) + I_{st}(t)$). The values are given as $E_{st} = 0.79 * D_{st}$ and $I_{st} = 0.21 * D_{st}$ (Maus & Weidelt 2004; Olsen, Sabaka & Lewes 2005).

The last line of equation (3) uses geocentric solar magnetospheric (GSM) coordinate system. It shows contributions from far magnetospheric current systems (e.g. tail currents). The functions R_n^0 are modification of Legendre functions to account explicitly for the induced field contributions due to the wobble of the GSM Z-axis with respect to the Earth's rotation axis. For a non-conducting earth,

these functions would be $R_n^0 = \left(\frac{r}{a}\right)^n P_n^0(\cos\theta_{GSM})$

where θ_{GSM} is colatitude in the GSM coordinate system (Maus & Luhr 2005).

RESULTS:

We use above three models to obtain the geomagnetic field estimates on the ground, during vernal equinox. Instead of taking entire field, which comprises the summation of the internal and external contributions, we consider the internal and external magnetic field separately.

Internal magnetic field:

The first term of equation (1) and (2), which is $\left(\frac{a}{r}\right)^{n+1}$ dependant term, gives the internal magnetic field that originates inside the earth. As discussed in the first section, the magnetic field coming from inside the earth comprises mainly two parts, viz., main field and crustal field. Normally, the coefficients up to degree 15 gives the main magnetic field with its source in the Earth's core, while expansion to degrees higher than 15 gives field of crustal origin. This crossover degree is based on the power spectrum of the main field model derived from Magsat data by Langel & Estes (1982), where the rate of change of the power spectrum changes abruptly somewhere between 14 and 16. Therefore, the internal field of each magnetic field

model can be separated into a core field (harmonics of degree 1-15), with its secular variation, and a lithospheric field (degree > 15). This indicates that higher the degree of expansion of the internal field (more than 15), better is the representation of the crustal contribution. For the exclusive crustal and lithospheric modelling, the spherical harmonic expansion of the scalar magnetic potential extends up to order 100 or more, and first 15 coefficients are set to zero in order to minimize the main field effect originating at the outer core.

The maximum degrees of spherical harmonic expansion achieved in all three geomagnetic field models studied here are displayed in Table 1.

Geo-magnetic field Model	Max degree of Internal field	Max degree of Secular field	Max degree of External field
CHAOS	50	18	2
CO2	49	13	2
OIFM	13	8	2

Note that the spherical harmonic expansion of internal field for CHAOS and CO2 model extends up to degree 50 and 49 respectively, whereas that for OIFM model is only up to order 13. This means that OIFM accounts only for the main field, i.e. core field; on the other hand the CHAOS and CO2 models, to some extent, could account for the magnetic field variations of the crustal origin. Nevertheless, the degree of expansion in CHAOS model does not go beyond 50, therefore it could only account for the longer wavelength magnetic field, which essentially comes from the lower crust. On the contrary, other exclusive lithospheric models are capable of accounting for the shorter wavelength crustal anomalies as well, coming from the upper part of the crust. Although, one should note that the satellite based model predicted crustal anomalies are not in accordance with the ground or aeromagnetic field data (Hemant et al., 2007) and hence are not competent to produce the finer details of the crustal anomalies just beneath the earth.

In this sub section, we compute the internal magnetic field on the surface of the earth, using geomagnetic field models discussed in the previous section. Since the values of the internal magnetic field are of the order of few ten thousands of nT, the differences of few hundreds of nT are not discernable. Therefore, just the model outputs do not assist

anymore in highlighting the disparity between the internal field obtained from the various models. Therefore, in order to compare the estimates of the internal magnetic field of all three models, we study 'the difference', by subtracting the internal magnetic field of OIFM and CO2 models from that of the CHAOS model.

Figure 1 shows the contour diagram of the difference between the internal magnetic field estimates obtained from the CHAOS and OIFM. Figures 1(a), (b), (c) and (d) represent the differences in X, Y, Z and F components respectively. Horizontal axis shows the geographic longitude; and Y-axis shows the geographic latitude ranging from 40°S to 40°N. Note that the colour bar is different for each figure, and it is shown on the right side of each figure.

As stated before, the internal part of the OIFM accounts only for the main field part, whereas CHAOS considers lower crustal field along with the main field, therefore the difference between CHAOS and OIFM can be believed to be due to the lower crustal magnetic field anomalies. From the figure, it is noticed that the difference varies from zero to few hundreds of nT's at certain locations. It is observed from Fig. 1(a) and (c) that the differences in X and Z-components are relatively larger compared to that in the Y component [Fig. 1(b)]. The differences in the total field (F) [see Fig.1(d)] shows three distinct longitudinal belts – one between 50°E and 100°E characterized by negative difference; second between 250°E and 300°E exhibiting positive difference; and third belt between 150°E and 250°E longitudes with almost zero difference between CHAOS and OIFM. This indicates that the lower crustal magnetic field is negative in the Indian region, and positive in the American zone. In the region between 150°- 250°E longitude the match between the two models is good, which may suggests that the contribution due to the higher order coefficients ($13 < \text{degree} \leq 50$) in the CHAOS model is very small. As stated earlier, the magnetic field evaluated from the higher degrees have crustal origin, therefore present observation may indicate that the magnetic field coming from the lower crust is close to zero in the region between 150°- 250°E longitude.

Well-known Bangui crustal anomaly, with bipolarity is one of the world's largest anomalies. It covers two third of the Central African Republic and the name derives from the capital city Bangui, that is near the center of this feature. In Figure 1, in the

African zone near the equator, this anomaly (highlighted in the rectangle) is very well seen. This substantiates the description that the difference between CHAOS and OIFM, is indeed due to the crustal field. The cause of the Bangui anomaly is controversial. Girdler, Taylor & Frawle [1992] proposed that this anomaly was produced by a large meteorite impact at one billion years old. Others have suggested it results from a major fracturing of the crust or the emplacement of a large igneous body.

Figure 2 shows the total internal magnetic field difference between CHAOS and CO2 model. From the magnitude of the colour bar shown on the right hand side, it is clear that the difference between these two models is small compared to that between CHAOS and OIFM. Although the difference is not zero, as one would expect it to be zero due to the fact that the internal field expands up to almost same degree in both the models (see Table 1). Therefore, the discrepancy is solely due to the intrinsic model differences.

Ring current:

As stated in the first section, the external magnetic field is due to the magnetospheric currents as well as due to its induced counter parts. The horizontal magnetic field estimates due to the ring current obtained from OIFM, CO2 and CHAOS models are depicted in figure 3(a), 3(b) and 3(c) respectively. The

terms dependent on $\left(\frac{r}{a}\right)^n$ in equations (1), and (2) are used for the ring current contribution from OIFM and

CO2 models, while $\left(\frac{r}{a}\right)^n$ dependent term in the first

and second lines of equation (3) are used for the CHAOS ring current. Since these calculations are Dst index dependent, we fixed the value of Dst to -100 nT. These magnetic field values are computed on the surface of the earth.

Figure 3 demonstrates that on the surface of the earth, the horizontal magnetic field component due to the ring current is always negative, suggesting that the ring current is westward. Since the ring current flow in the equatorial plane, its effect is stronger in the vicinity of the equator. From Fig.3, it is observed

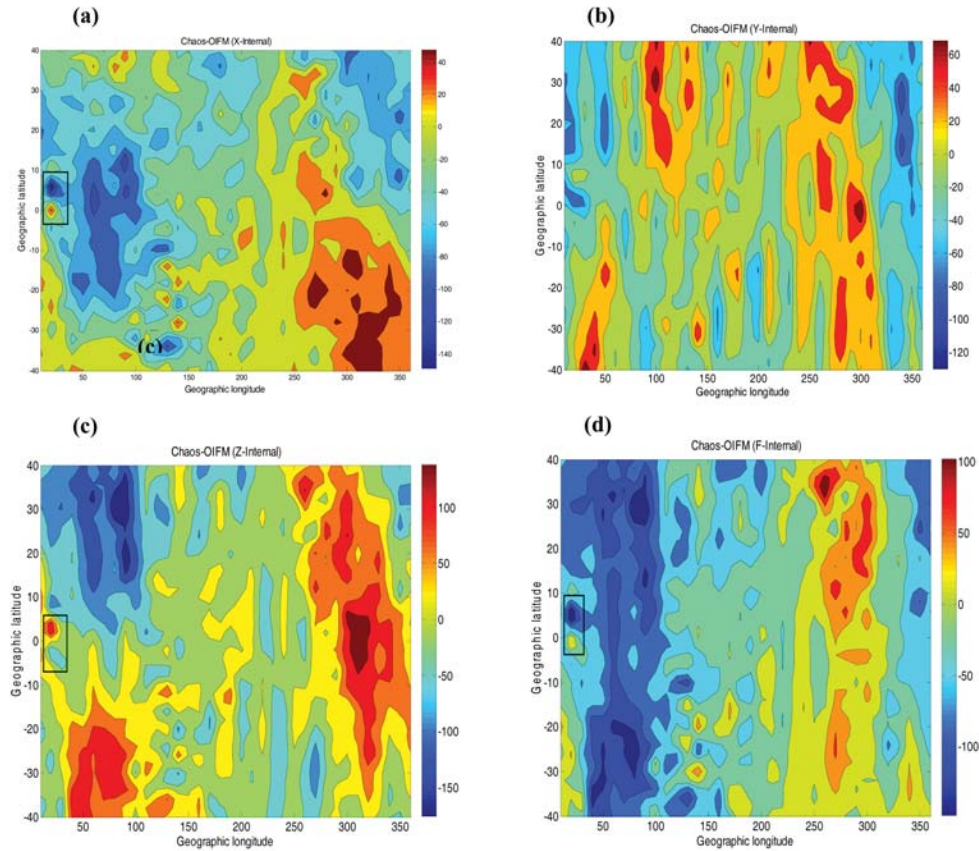


Figure 1. Difference between the internal magnetic field estimates obtained from CHAOS and OIFM on the surface of the Earth. (a) X- component, (b) Y- component, (c) Z- component, and (d) F- component. X- axis shows the geographic longitude and Y-axis indicates the geographic latitudes. The color code for each contour plot is shown on the right hand side.

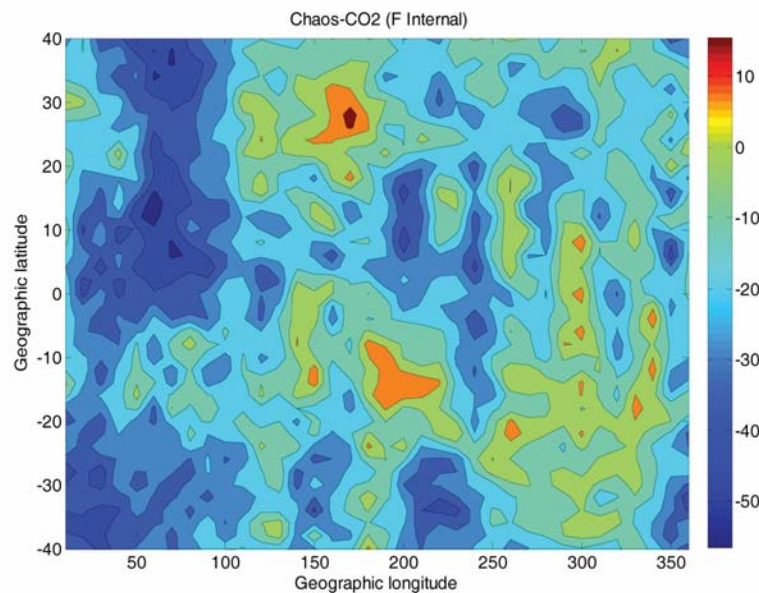


Figure 2: Difference between total internal magnetic field (F component) obtained from CHAOS and CO2 model, on the surface of the earth.

that the OIFM gives stronger magnetic field compared to other two models. Therefore the satellite data based investigation of the ionospheric current systems such as equatorial electrojet, solar quiet time currents etc. using OIFM may subtract larger ring current contribution, which may result in the weaker estimates of the ionospheric currents. Further, recall from the equation (1) that the ring current computation for OIFM, is performed in the geographic coordinate system, and hence the ring current flowing in the geographic equatorial plane gives the magnetic field variations symmetric about the geographic equator. On the other hand, the dipole coordinate system is used for the CHAOS and CO2 model, and consequently the ring current flows in the geomagnetic equatorial plane. Therefore figures 3(b) and 3(c) are not symmetric about the geographic equator. In figure 3(d), we show the zonal variation of the geographic latitude of the geomagnetic equator. Now comparing the symmetry of the ring current contribution in CO2 and CHAOS, we notice that the magnetic field is almost symmetric about the geomagnetic equator.

Induced current:

Figure 4 shows horizontal component of the induced magnetic field due to the magnetospheric ring current. The induced field is determined by factor Q_1 in OIFM and CO2 models (equations 1 & 2), and the factor $\left(\frac{I_{st}}{Dst}\right)$ in CHAOS model (equation 3). This controlling factor has value of 0.27, 0.28 and 0.21 in OIFM, CO2 and CHAOS models respectively. Therefore, the induced current contribution is less in CHAOS model (figure 4(c)), compared to other two models. Again in Fig.4, it is evident that the induced current is virtually symmetric about the geographic equator in the OIFM (figure 4(a)), while in other two models it is symmetric about the geomagnetic equator [Fig.4(b) & Fig.4(c)]. Now using figures 3 and 4, compare the magnitude of the magnetic field estimates due to the ring current and induced current in each model. It is perceived that in general, the ring current contributions are about five times stronger than that of due to the induced currents.

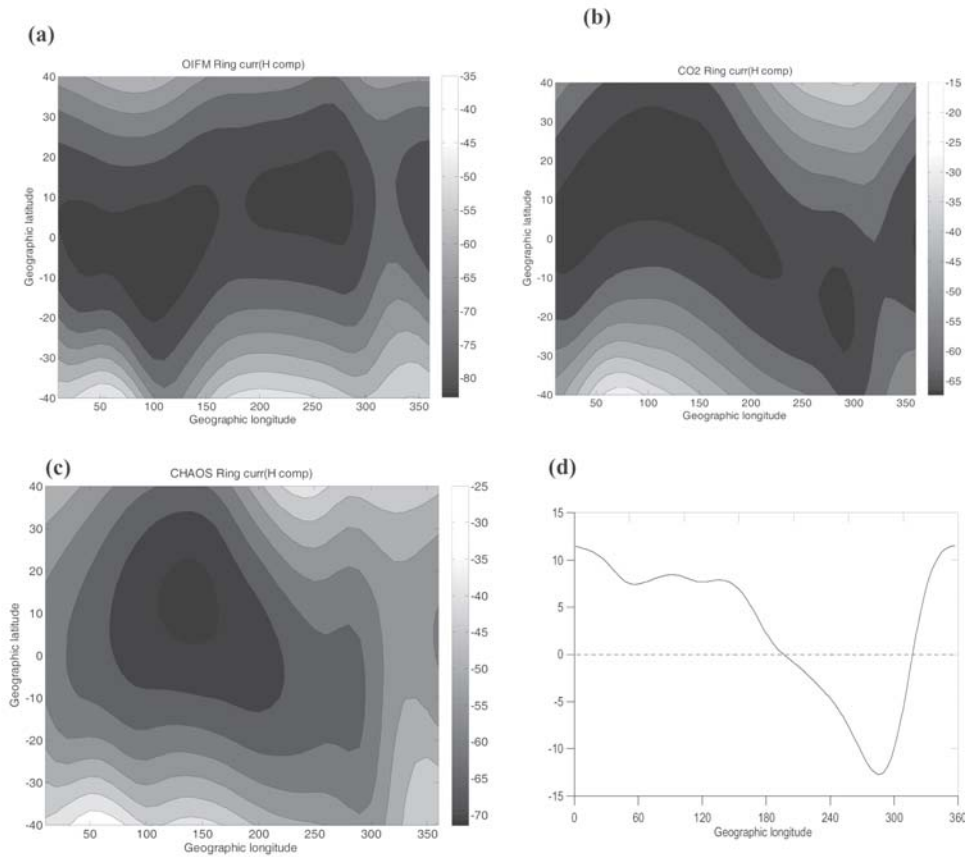


Figure 3. External magnetic field (horizontal component) due to ring current ($Dst = -100$ nT), on the surface of the earth, obtained from (a) OIFM, (b) CO2, and (c) CHAOS models. Figure (d) shows the zonal variation of the geographic latitude of the geomagnetic equator.

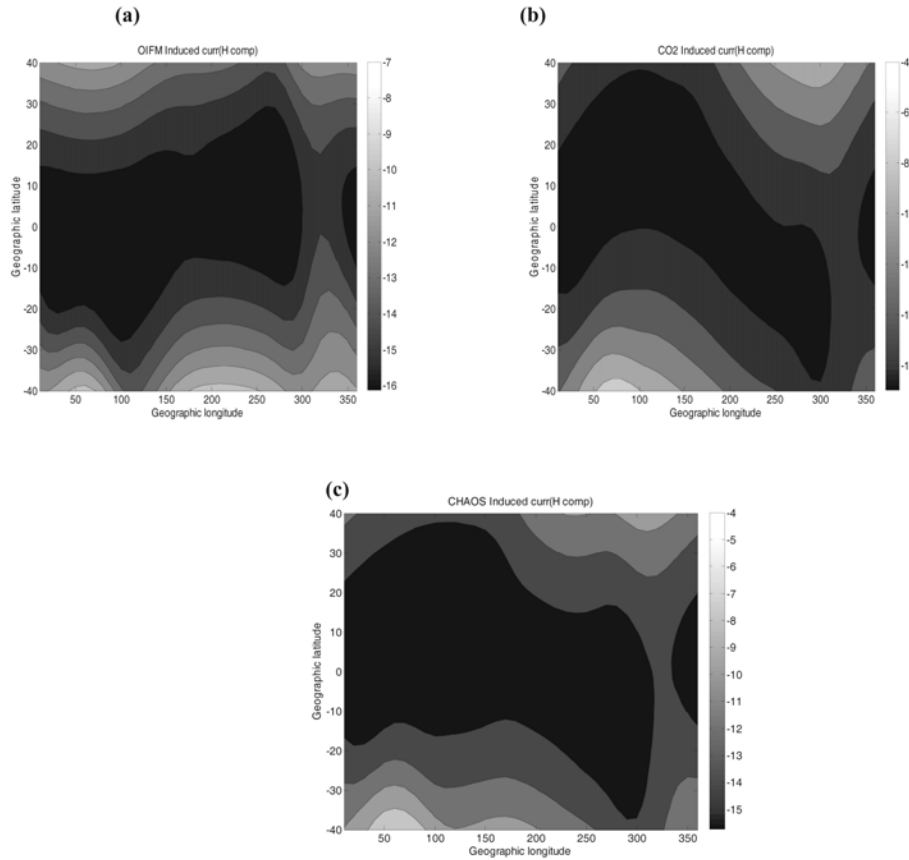


Figure 4. Horizontal magnetic field at the surface of the earth due to induced ring current ($Dst = -100$ nT), obtained using (a) OIFM, (b) CO2, and (c) CHAOS models.

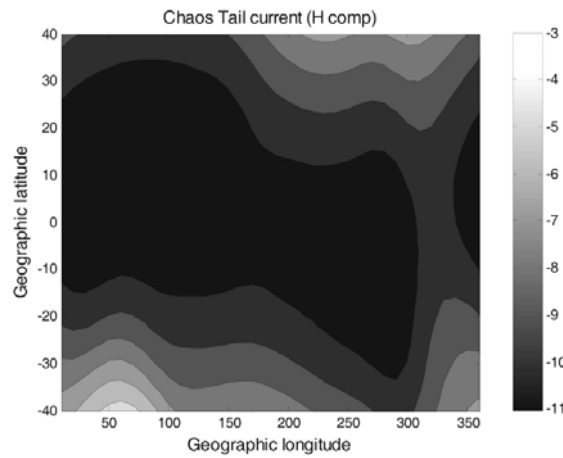


Figure 5. Horizontal component of the external field due to tail current obtained from CHAOS model.

Tail current:

Only CHAOS model accounts for the magnetic field variations due to the tail current flowing in the magnetotail region. Note that to evaluate the effect of tail current, last term of equation 3 employs

geocentric solar magnetospheric (GSM) coordinate system. Figure 5 shows the tail current estimates obtained from the CHAOS model. It is observed that it is always negative, suggesting that the tail current produces depression in the horizontal component of the magnetic field on the ground.

Also note that the magnitude of the magnetic field due to the tail current is very small compared to that of due to the ring or induced current. It is weak all over the globe. One should also notice that the difference in the magnitude of the magnetic field from mid to low latitude is very less (~ 4 nT), indicating that the tail current is almost same everywhere. This is expected because of the fact that the tail current flows in the magnetotail, which is situated at a distance of ~ 100 - $200 R_E$ from the earth. Therefore, due to its far location, its influence on the surface of the globe is almost same.

CONCLUSIONS

For the investigation of the ionospheric current system using satellite based observations, it is necessary to remove the earth's magnetic field values. Availability of number of geomagnetic field models puzzles the researchers in choosing the appropriate model. Different geomagnetic field models may give rise to different estimates of the ionospheric currents. Hence in order to get an idea of how much the results can vary due to the use of different field models, we embark the present comparison between various geomagnetic field models.

In the present work, we compare CHAOS model, which is the most recent long-term model of Earth's magnetic field with earlier epoch based models such as Oersted Initial Field Model, (OIFM) and CO2 model. The CHAOS model uses magnetic field measurements obtained from Oersted, CHAMP and SAC-C satellites. The CO2 model utilizes all three satellites as well as ground observatory data, whereas OIFM uses single satellite observations. The internal magnetic field expands to higher spherical harmonics (degree ~ 50) in the CHAOS and CO2 models, compared to that in the OIFM (degree = 13). The expansion in OIFM is just sufficient for the main field inclusion, while CHAOS and CO2 do account for the crustal magnetic field as well. Since the expansion does not extend to higher spherical harmonics up to or more than 100 degrees, these models can produce only longer wavelength crustal anomalies, which originate in the lower crustal region.

Therefore the difference in the Internal field (Core + Crustal) between CHAOS and OIFM can be treated as due to the crustal field, particularly lower crustal field. The difference displays three distinct longitudinal belts – one in the Indian region with negative lower crustal field, second in the American zone of positive lower crustal field, and third region between 150° - 250° E longitude, where the match between the two models is good.

This could indicate that the longer wavelength magnetic field contribution coming from the lower crust is minimum in the region between 150° - 250° E longitude. Well-known Bangui crustal anomaly in the central African region is also evident in Fig.1.

The present work estimates the ring current and induced current contribution from all three models, and tail current from CHAOS model. The magnetic field estimates due to the ring current are about five times stronger than that of due to the induced current. The OIFM is found to produce stronger ring current effect on the ground compare to other two models. This could result in the underestimated ionospheric currents using OIFM. Further, due to the difference in the coordinate systems used in various models, the symmetry of the magnetic field is different. In the OIFM, ring current field is symmetric about the geographic equator, whereas in CO2 and CHAOS models it is symmetric about the geomagnetic equator.

The tail current contribution from CHAOS model seems to be weakest and same almost everywhere on the globe due to its far location.

ACKNOWLEDGEMENT

Authors would like to thank GFZ Helmholtz Centre, Potsdam for making available the coefficients of geomagnetic field models.

REFERENCES

- Chapman, S. & Bartels, J., 1940. Geomagnetism, Vols. I and II, Oxford University Press.
- Daglis, I.A. & Kozyra, J.U., 2002. Outstanding issues of ring current dynamics, *J. Atmos. Sol. Terr. Phys.*, 64, 253–264.
- Girdler, Taylor & Frawley, 1992., A possible impact origin for the Bangui magnetic anomaly, *Tectonophysics*, 212, 45-58
- Hemant Kumar, E., Thébault, M., Manda, D., Ravat, Maus, S., 2007. Magnetic anomaly map of the world: merging satellite, airborne, marine and ground-based magnetic data sets, *Earth and Planetary Science Letters*, 260, 56–71.
- Holme, R., Olsen, N., Rother, M. & Lühr, H., 2003. CO2: A CHAMP magnetic field model, in *First CHAMP Mission results for Gravity, Magnetic and Atmospheric Studies*, eds Reigber, C., Lühr, H. & Schwintzer, P., p. 220–225, Springer Verlag, Berlin-Heidelberg-New York.
- Jadhav, Geeta, Rajaram, M. & Rajaram, R., 2002. Main field control of the equatorial electrojet: a preliminary study from the Oersted data, *J. of Geodynamics*, 33 (1-2),

- 157-171.
- Langel, R. A. & Estes, R.H., 1982. A geomagnetic field spectrum, *Geophys. Res. Lett.*, 9, 250-253.
- Langel, R. A. & Estes, R.H., 1985. The near-Earth magnetic field at 1980 determined from MAGSAT data, *J. Geophys. Res.*, 90, 2495-2509.
- Maus S. & Kuvshinov, A., 2004. Ocean tidal signals in observatory and satellite magnetic measurements, *Geophys. Res. Lett.*, 31, L15313, doi:10.1029/2004GL020090.
- Maus, S. & Weidelt, P., 2004. Separating the magnetospheric disturbance magnetic field into external and transient internal contributions using a 1D conductivity model of the Earth, *Geophys. Res. Lett.*, 31, L12,614, doi:10.1029/2004GL020, 232.
- Maus, S. & Lühr, H., 2005. Signature of the quiet-time magnetospheric magnetic field and its electromagnetic induction in the rotating Earth, *Geophys. J. Int.*, 162, 755-763.
- Maus, S., Rother, M., Hemant, K., Stolle, C., Luehr, H., Kuvshinov, A. & Olsen, N., 2006. Earth's lithosphere magnetic field determined to spherical harmonic degree 90 from CHAMP satellite measurements. *Geophys. J. Int.* 165 (2), 319-330.
- Maus, S., Luehr, H., Martin, R., Hemant, K., Balasis, G., Ritter, P. & Claudia, S., 2007. Fifth-generation lithospheric magnetic field model from CHAMP satellite measurements. *Geochem. Geophys. Geosyst.* 8, Q05013. doi:10.1029/2006GC001521.
- McCreadie, H. & Iyemori, T., 2006. Equatorial electrojet as a diagnostic tool of geomagnetic field models, *Earth Planets Space*, 58,885-893
- Olsen, N. et al., 2000. Ørsted initial field model, *Geophys. Res. Lett.*, 27, 3607-3610.
- Olsen, N., Sabaka, T.J. & Lowes, F., 2005. New parameterization of external and induced fields in geomagnetic field modeling, and a candidate model for IGRF 2005, *Earth, Planets and Space*, 57, 1141-1149.
- Olsen, N., Lühr, H., Sabaka, T.J., Manda, M., Rother, M., Toffner-Clausen, L. & Choi, S., 2006. CHAOS — a model of the Earth's magnetic field derived from CHAMP, Ørsted, and SAC-C magnetic satellite data. *Geophys. J. Int.* 166 (1), 67-75.
- Sugiura, M., 1964. Hourly values of the equatorial Dst for the IGY, *Ann. IGY*, 35, 9-45.

(Revised accepted 2008 December 28; Received 2008 November 17)



Dr. Geeta Vichare presently working at Indian Institute of Geomagnetism, Mumbai, obtained her Master of Science degree in Space Physics from Pune University and subsequently Ph.D. degree from Mumbai University in 2002, under guidance of Prof. R. Rajaram. During her doctorate, she worked on Oersted satellite data, Ionospheric conductivity, Atmospheric tides, Micropulsations and Numerical Model of Equatorial Electrojet. Then she joined High Altitude Observatory (HAO), NCAR, Boulder, USA, as a Post Doctoral Fellow, where she worked with Prof. A.D. Richmond on NCAR's Magnetosphere-Thermosphere-Ionosphere-Electrodynamics General Circulation Model. Currently she is involved in satellite and ground data based research and also on the theoretical modeling of the low latitude current system. So far she has published over 10 research paper in various reputed scientific journals. She has worked as a reviewer for four research papers submitted to JGR- Space; and two papers submitted to EPS and International Journal of Geomagnetism and Aeronomy.



Prof. R. Rajaram is a Ph.D. in Plasma Physics of Delhi University. Along with his students he has been involved in research on various aspects of space and atmospheric physics for over forty years. He has published numerous papers in National and International Journals of repute. In addition to his long research career at Indian Institute of Geomagnetism in India, he has also worked at, GSFC NASA and Applied Physics Laboratory of The Johns Hopkins University in USA and the Geophysical Institute of Kyoto University in Japan. He is currently Advisor on New Technology and Intellectual Property Issues for Micro Technologies (India).